

# **In situ Temperature Evolution and Failure Mechanisms of LiNi<sub>0.33</sub>Mn<sub>0.33</sub>Co<sub>0.33</sub>O<sub>2</sub> Cell under Over-Discharge Conditions**

Linmin Wu, Yadong Liu, Yi Cui, Yi Zhang, Jing Zhang\*

Department of Mechanical Engineering, Indiana University-Purdue University Indianapolis,  
Indianapolis, IN 46202, USA

\*Email: jz29@iupui.edu; Phone: 317-278-7186; Fax:317-274-9744

## **Abstract**

In this work, in situ study of commercial 18650 NMC (LiNi<sub>0.33</sub>Mn<sub>0.33</sub>Co<sub>0.33</sub>O<sub>2</sub>) cells under over-discharge charge conditions (100%, 110%, and 120%) has been performed. Both voltage and cell skin temperature evolutions were simultaneously monitored in situ during discharge process. The results show that there is a clear correlation between the voltage and temperature. For the NMC cell under 120% over-discharge condition, the cell failed after only 1 cycle. The voltage dropped to negative values at the end of the discharge. The skin temperature at the end of discharge increased dramatically to 73 °C, indicating strong exothermal reactions happened inside the cell. For the 110% over-discharged cell, the cell failed after 10 cycles. The voltage at the end of the discharge process became negative after the 1st cycle. The cell skin temperature increased from 23.2 °C to 61.7 °C. The peak temperature in each cycle kept increasing until failure. These implies the micro short circuits were developed during the charge-discharge process. The failed components were examined by SEM/EDX and XRD. The results show substantial aluminum exists inside the failed separators. The results suggest that during the over-discharge process, the alumina

---

This is the author's manuscript of the article published in final edited form as:

Wu, L., Liu, Y., Cui, Y., Zhang, Y., & Zhang, J. (2018). In Situ Temperature Evolution and Failure Mechanisms of LiNi<sub>0.33</sub>Mn<sub>0.33</sub>Co<sub>0.33</sub>O<sub>2</sub> Cell under Over-Discharge Conditions. *Journal of The Electrochemical Society*, 165(10), A2162–A2166. <https://doi.org/10.1149/2.0791810jes>

inside the separator was reduced to aluminum. The electrons migrate through aluminum channel, leading to the failure of the cells.

**Key words:** failure; over-discharge; NMC, in situ, temperature

## 1. Introduction

Lithium ion rechargeable batteries (LIBs) are desirable for electronic devices, electric vehicles (EVs) and hybrid electric vehicles (HEVs) because of their long cycle life, high energy density and high efficiency [1, 2]. However, abnormal operations and extreme environment can cause serious safety issues. Recently, many safety accidents regarding LIBs have been reported: thousands of Lenovo laptops have been recalled because of the thermal runaway problems of LIBs [3]. Tesla EVs caught 4 fire accidents in 6 weeks [4]. The battery packs of Boeing 787 caught fire after grounding [5]. These accidents brought great public concerns. Thus, it is important to have a deep understanding of the failure mechanisms of LIBs.

Many efforts have been given to investigate the abuse operations of LIBs. Studies have been done to thermal abuse [6-8], mechanical abuse [9-11], and electrical abuse [12-14]. Among electrical abuse, more attentions have been attracted to the overcharge tests, since overcharging can cause hazardous situations, such as gas generation, high temperature and even explosion. However, few works have been done to focus on the failure mechanisms of LIBs under over-discharge conditions. Zheng et al. [15] evaluated the over-discharge performance on the  $\text{LiFePO}_4$ /graphite cells. They found significant impedance increase inside the cells after the over-discharge tests accompanied with 24.55% capacity loss. Tobishima et al. [16] abused the  $\text{LiCoO}_2$  and  $\text{LiMn}_2\text{O}_4$  batteries under 250% over-discharge condition. The cells were observed to fail after 1 cycle, but the failure mechanism is not clear. He et al. [17] proposed the failure mechanism of over-discharge tests that copper in the anode current collector could be oxidized into ions in the over-discharge process and then redeposited as copper metal at the electrode. The migration of copper might penetrate the separator and cause internal short circuits.

During the over-discharge process, the temperature will arise due to the exothermal reactions inside the cell [17]. At high temperatures, the anode solid electrolyte interface (SEI) layer may break down [18, 19], leading to capacity loss and failure of the cell. Almost all the reported failure of the LIBs under over-discharge condition started from the copper dissolution and migration. However, the copper dissolution and deposition is not observed in this study. To our best knowledge, an in situ study of temperature evolution and failure mechanism related to aluminum formation in separator has not been reported yet. Here, we report the aluminum formation in separator is the main failure mechanism of commercial LG 18650 NMC cells under over-discharge conditions.

In this paper, the over-discharge effect on commercial 18650 NMC cells is studied. The paper will be organized as follows: In section 2, the details of experimental method are described. In section 3, the cycling performance and the temperature response of the NMC cells under normal, 110% and 120% over-discharge are analyzed. The microstructure changes after the tests are studied using SEM/EDX and XRD. The failure mechanism is also discussed. Conclusions are given in section 4.

## **2. Experimental**

### **2.1 Materials**

The commercial cells used in this study is LG 18650 cells (LGDBHE41865). The cathode is  $\text{LiNi}_{0.33}\text{Mn}_{0.33}\text{Co}_{0.33}\text{O}_2$  (NMC), and the anode is mesocarbon microbeads (MCMB) graphite. The normal operating potential is between 2.0 V (0% state of charge) and 4.2 V (100% state of charge). The nominal capacity is 2500 mAh.

## 2.2 Over-discharge cycling tests

Over-discharge tests were carried out in a homemade explosion-proof chamber using both the BT-5000 8-channel battery and the BT-2000 32-channel cycler with a temperature-control sensor (Arbin Instruments, TX). Galvanostat tests were performed on the LG 18650 NMC cells with a nominal 2500 mAh capacity. The cells were charged to 4.20 V at 1 C rate (constant current of 2.50 A) first; then, the charging was continued at a constant voltage of 4.20 V until the current was  $< 0.02$  A, which is regarded as a 100% state of charge (SOC) or 0% depth of discharge (DOD). After a short rest (i.e. 5 min.), the cell was discharged at 1 C rate until the voltage reached 2.0 V, which is the discharge cutoff voltage of the cell (the corresponding capacity is 2500 mAh). This procedure is considered to be a 100% depth of discharge (DOD). The over-discharge test conditions were carried out at 1 C rate (constant current, 2.50A) and based on the Coulombs discharged out of the cell; namely, the discharge step was terminated when the cells reach 110% DOD (66 min., 2750 mAh) and 120% DOD (72 min., 3000 mAh) instead of 2.0 V while the cell voltage went negative at the end of over-discharge. A thermocouple was placed on the skin of the LG 18650 NMC cell in the middle of the cell and the in situ temperature was measured simultaneously with the voltage during the cycling test. The charge/over-discharge cycles kept running until the cells failed.

## 2.3 Scanning electron microscope (SEM), energy-dispersive X-ray spectroscopy (EDX) and X-ray diffraction (XRD) characterization of 18650 NMC cells

The normal and failed cells were carefully disassembled in the argon filled glove box after the cycling of the cells. The cathodes, anodes and separators of the cells were cut off from the disassembled cells for further examinations. The XRD patterns were collected on a Bruker D8 Discover XRD Instrument equipped with Cu  $K\alpha$  radiation (wavelength=1.5405 Å). The samples

were washed by DMC completely to remove lithium salts before the measurements. The samples were protected in the sample holder with Kapton film. The scanning rate was  $2^\circ \text{ min}^{-1}$ , and  $2\theta$  was set between  $10^\circ$  and  $80^\circ$ . The morphology was examined by JEOL JSM-7800F field emission scanning electron microscopy. The elemental scans were conducted using energy-dispersive X-ray spectroscopy attached to the SEM with 15 KV.

### 3. Results and discussion

#### 3.1 Behaviors of over-discharged 18650 NMC cells

The electrochemical performance of a LG 18650 NMC cell under normal charge-discharge cycles is shown in Fig. 1. The voltage and temperature curves are plotted for the first three cycles. For the constant current charging, the temperature increases  $5.2^\circ \text{C}$  for the first cycle and decreases  $4^\circ \text{C}$  to  $4.5^\circ \text{C}$  for the rest of two cycles. The temperature decreases  $5.1^\circ \text{C}$  for the first cycle and  $6^\circ \text{C}$  for the rest of two cycles during the constant potential process. There are large increases in temperature of about  $10.2^\circ \text{C}$  for the discharge process.

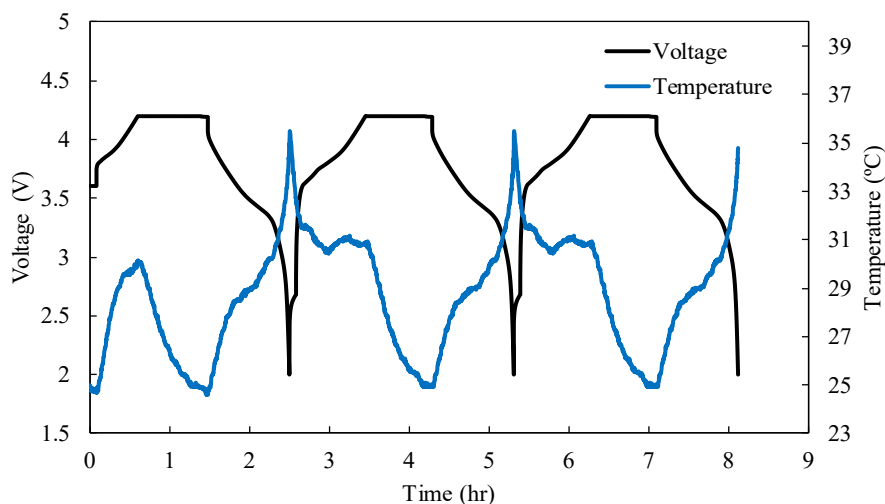


Fig. 1 Voltage and temperature curves of the 18650 NMC cell under normal charge-discharge cycles.

The cell was also cycled in over-discharge conditions. The voltage and temperature curves for the 120% over-discharge are shown in Fig. 2. There is a clear correlation between the voltage and temperature. The cell failed after only 1 cycle. During the over-discharge process, the voltage drops sharply from 2.0 V to -0.8 V, and then goes back to -0.16 V and maintains at -0.16 V. Meanwhile, the skin temperature increases dramatically to 73 °C for over-discharging. After the 120% over-discharge process, the cell was not able to charge, which means the failure of the cell. The large increase of temperature indicating strong exothermal reactions happened inside the cell. This phenomenon implies there might exist micro short circuit inside the cell. It can also be concluded that 120% over-discharge for 18650 NMC cells is extremely detrimental to the cycle performance.

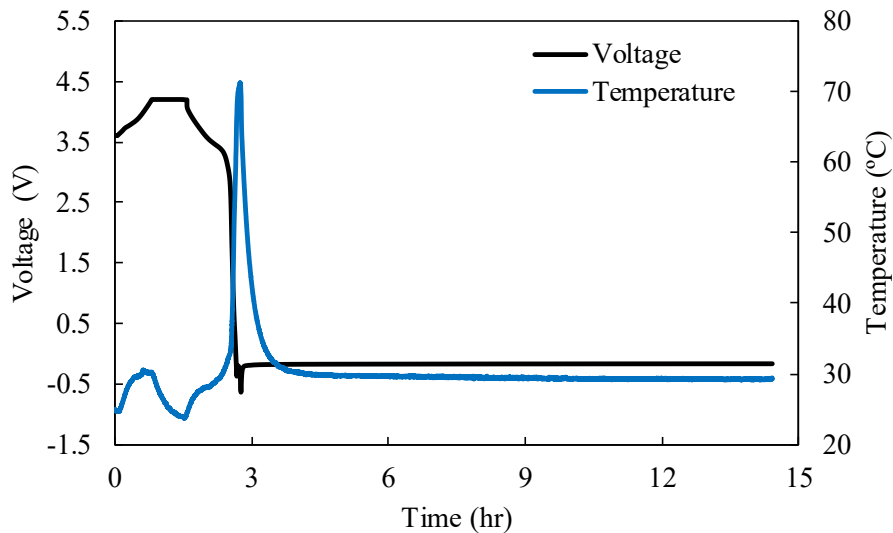
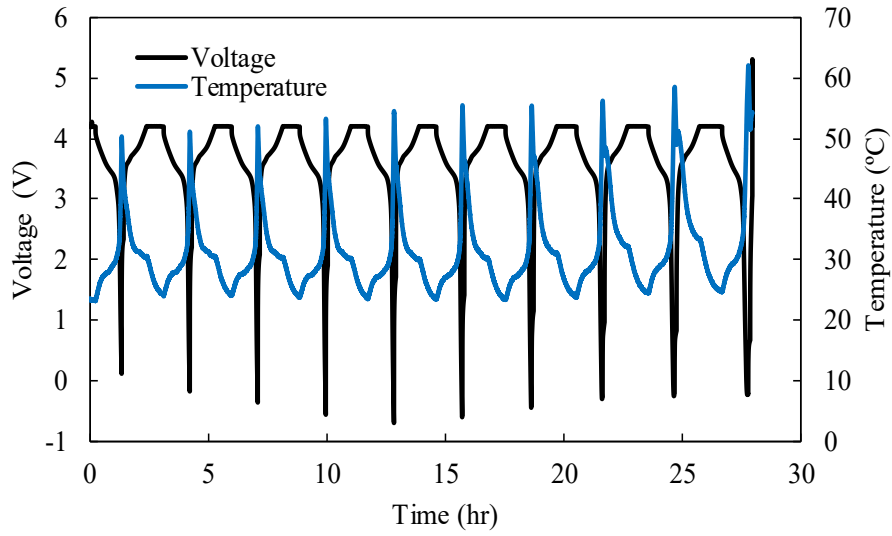


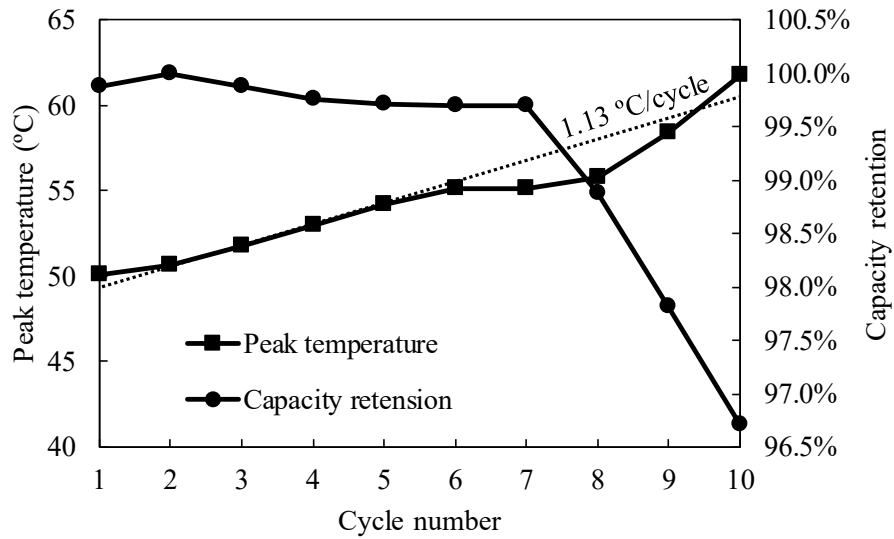
Fig. 2 Voltage and temperature curves of the 18650 NMC cell under 120% over-discharge condition.

Since the 18650 NMC cell under 120% over-discharge condition failed only after 1 cycle, it is hard to observe the performance change during the cycling. In order to monitor the electrochemical behavior change during the over-discharge process, the NMC cell under 110% over-discharge condition was also studied. The voltage response and monitored temperature for over-discharging is shown in Fig. 3a. Similar to the 120% case, there is a clear correlation between the voltage and temperature. The cell failed after 10 cycles. The voltage at the end of the discharge process becomes negative after 1<sup>st</sup> cycle. It decreases for the first 5 cycles, and reaches the minimum -0.81 V at the 5<sup>th</sup> cycle. And then, the voltage increases until the 10<sup>th</sup> cycle. At the end of the 10<sup>th</sup> cycle, the voltage is still negative, which is -0.21 V. After 10<sup>th</sup> cycle, the voltage increases dramatically to 5.62 V and the cell was unable to discharge, which implying the failure. The temperature evolution during the over-discharge condition is also shown in Fig. 3a. The temperature increases from 23.2 °C to 61.7 °C. The temperature at the end of discharge process, which is the peak temperature at each cycle, shows a trend of increase with a rate of 1.13 °C/cycle (see Fig. 3b), while the temperature at the end of the charging process has a much smaller increase speed, which is 0.16 °C/cycle. The peak temperature values and discharge capacity retention of the NMC cell are given in Fig. 3b. With the increase of the cycle number, the capacity retention decreases from 100% to 99.7% for the first 7 cycles, and then decreases sharply to 96.7% at the end of 10<sup>th</sup> cycle. Meanwhile, the peak temperature of the NMC cell increases sharply from 55.1 °C to 61.74 °C for 7<sup>th</sup> cycle to 10<sup>th</sup> cycle. The above observations suggest the micro short circuits formed under 110% over-discharge conditions, and strong exothermal reactions occurred inside the cell. With the increase of the cycling number, the micro short circuits were developing, which can cause further damage to the electrochemical performance.





(a)



(b)

Fig. 3 (a) Voltage and temperature curves of the 18650 NMC cell under 110% over-discharge condition. (b) Peak temperature and discharge capacity retention of the 18650 NMC cell under 110% over-discharge condition.

### 3.2 Characterizations of microstructures of cell components

In order to understand the microstructure changes of the cells under over-discharge conditions, the normal and failed components of cells were examined by SEM and EDX. There is no detectable difference in cathodes and anodes between the 100% discharged, 110% over-discharged and 120% over-discharged cells. However, the separators show distinctive features. The SEM images of the cross sections of 100% discharged, 110% over-discharged and 120% over-discharged cells are shown in Fig. 4, Fig. 5, and Fig. 6, respectively. For the separator under normal charge-discharge condition, the surface is quite smooth. Through elemental analysis for the selected area, the peaks of carbon in both areas are much higher than aluminum (see Fig. 4). The source of the Au is from the SEM exam for better conductivity. This can also be confirmed by the line scan analysis. The content of carbon is about 4 times the content of aluminum. Since aluminum was detected using EDX in normally cycled cell, it is possible that alumina was coated inside the separator during the manufacturing process. For the separator under 110% over-discharge condition, several pores were observed in the SEM image (Fig. 5). It is noted that the pores in the separator is typically around 50 nm in diameter, which is invisible in the length scale of several microns. Hence, the black spots were regarded as melted regions, which may be caused by the micro short circuits. The EDX area scan of the melted region (Fig. 5) show that the intensity of aluminum peak is much stronger than other peaks, indicating there are large amounts of aluminum inside the separator. It is also found that the content of aluminum is about 5 times the content of carbon. For the separator under 120% over-discharge condition, no melted regions were found as the 110% over-discharged sample. This may be because for 120% over-discharge, the cell failed after 1 cycle. The short circuit might be highly localized, and happened only at few selected locations. While for 110% over-discharge, the cell failed after 10 cycles. The short circuits developed with

the increase of the cycle number, leading to a uniform distribution of the melted spots. Similar to the 110% over-discharged sample, large amounts of aluminum were found inside the 120% over-discharged separator (see Fig. 6), and the content of aluminum is higher than carbon. Although EDX results can not show absolute contents of the elements, it can show the changes of relative contents. The relative amount of aluminum increases dramatically after over-discharging. It seems like something formed in the separator during over-discharging.

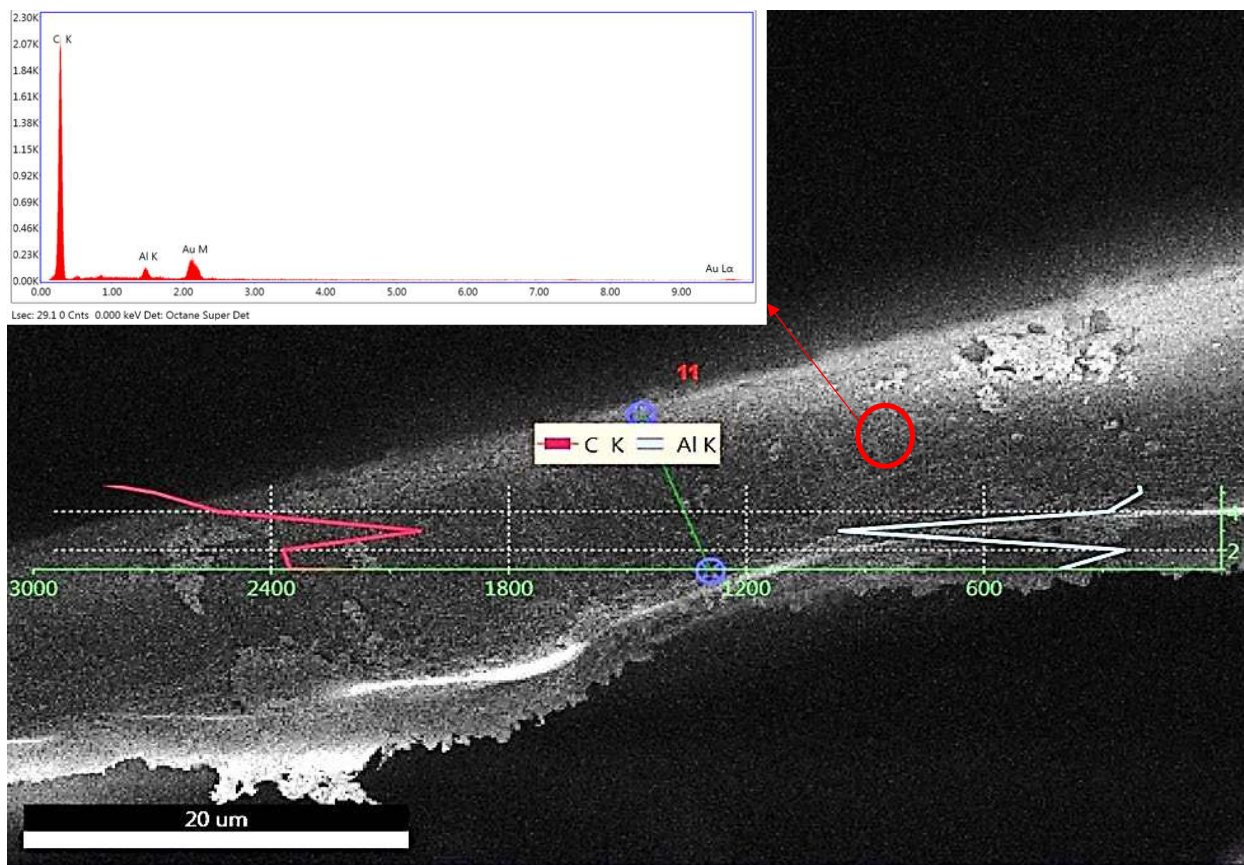


Fig. 4 SEM image of the separator under normal charge-discharge condition. EDX line and area scan results are shown in the image.

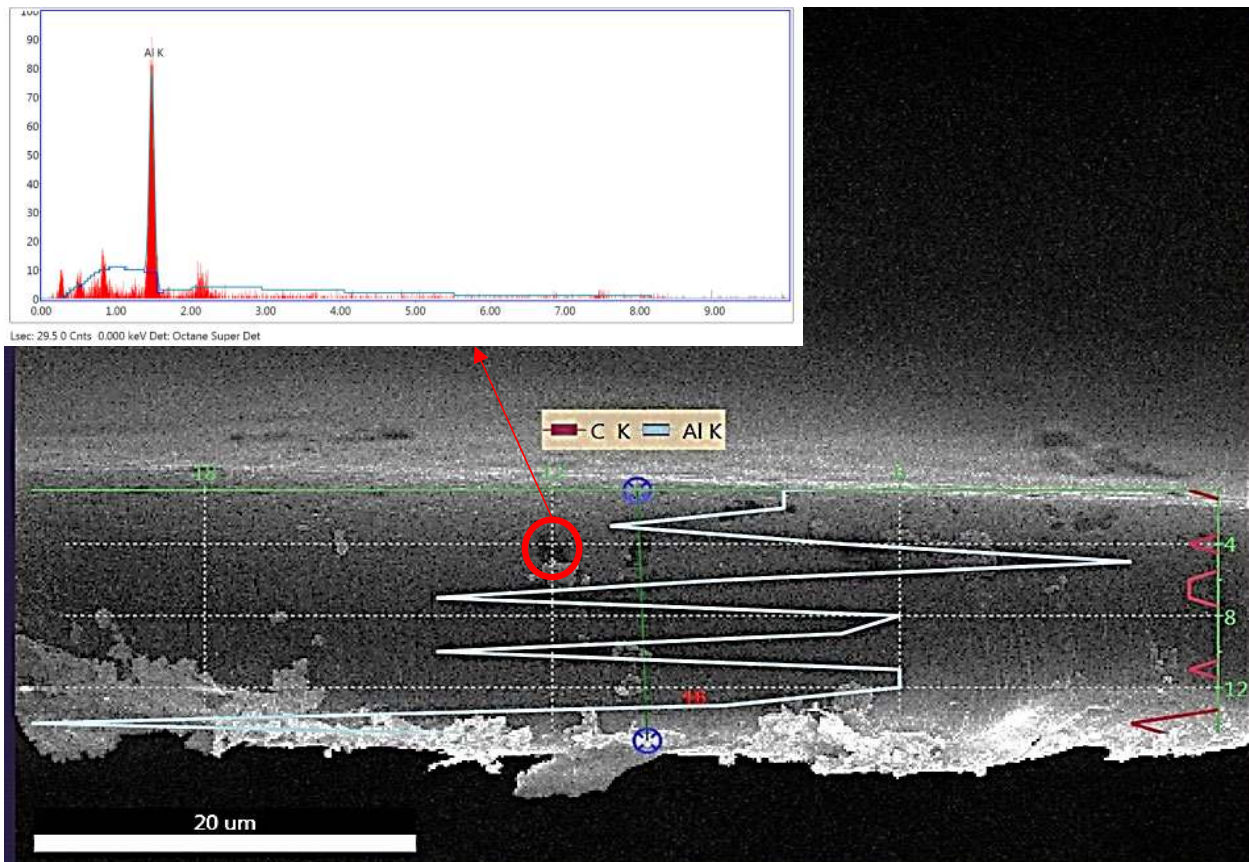


Fig. 5 SEM image of the separator under 110% over-discharge condition. EDX line and area scan results are shown in the image. The melted region is shown inside the red circle.

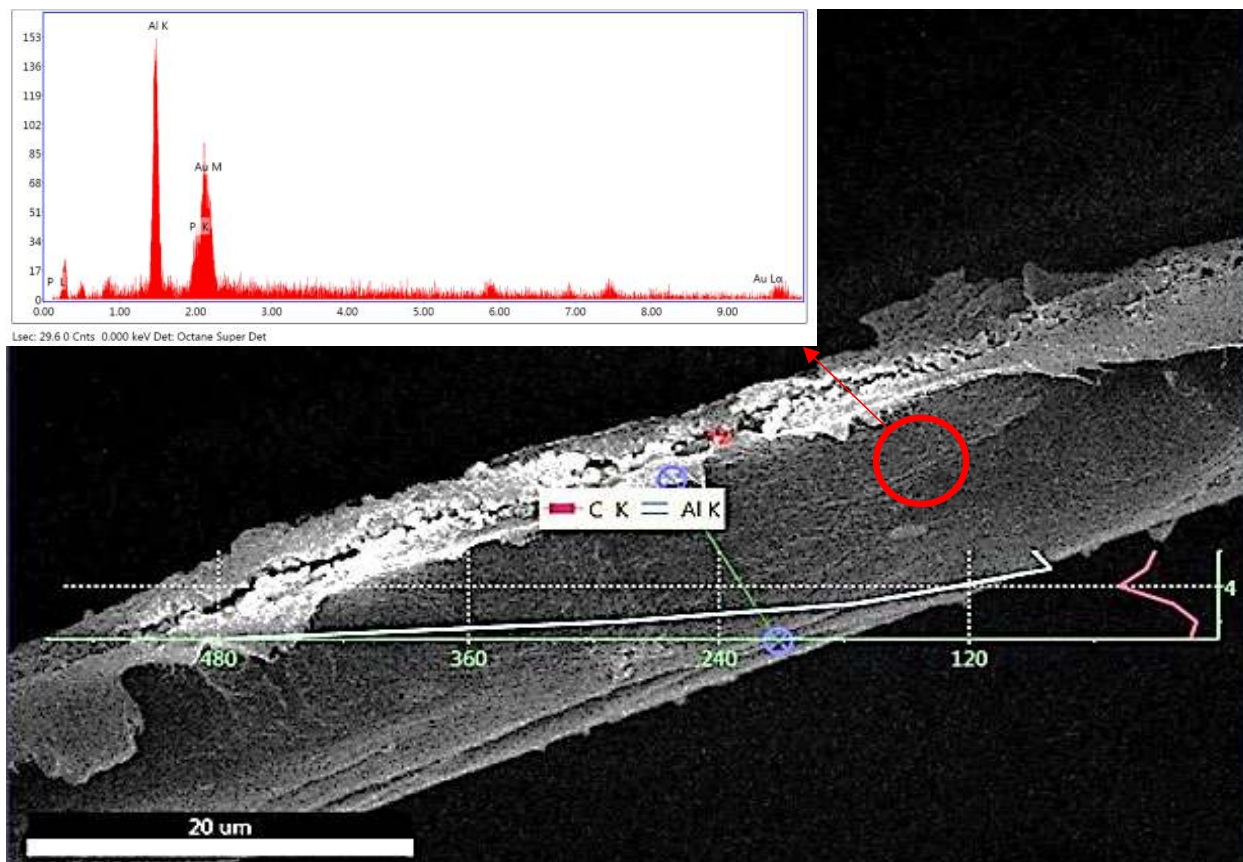
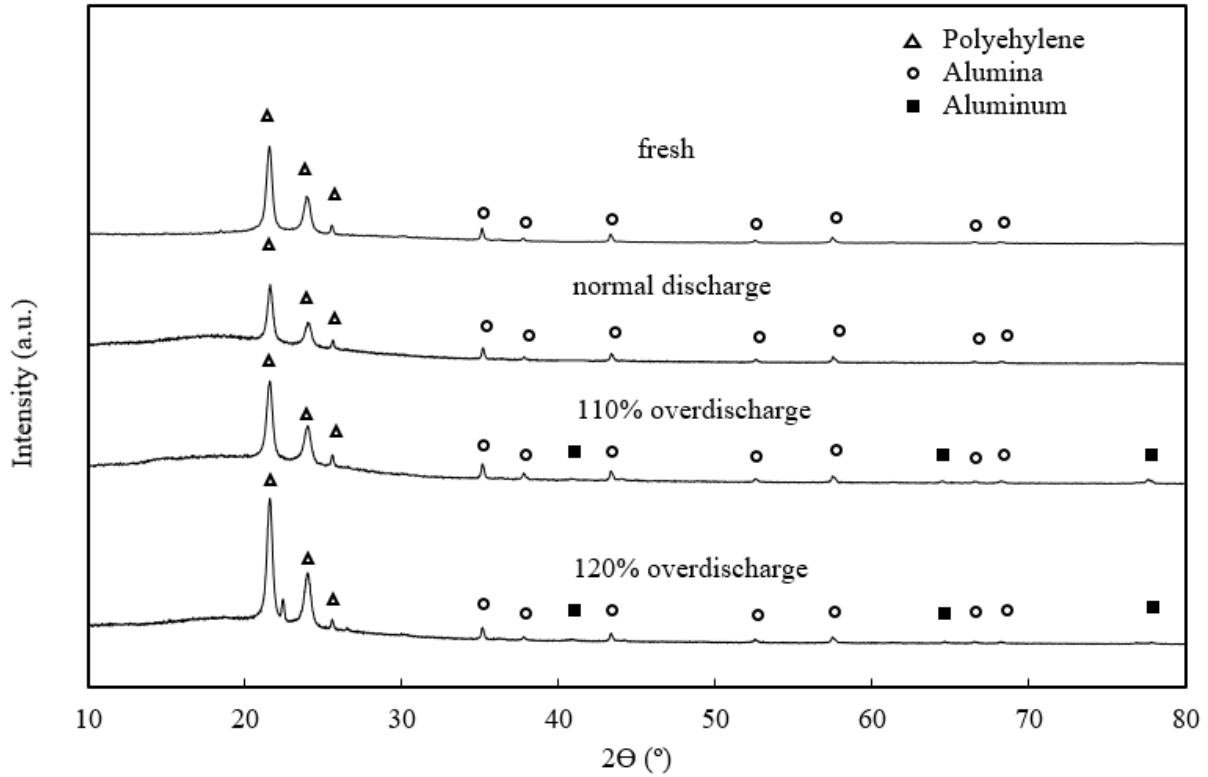


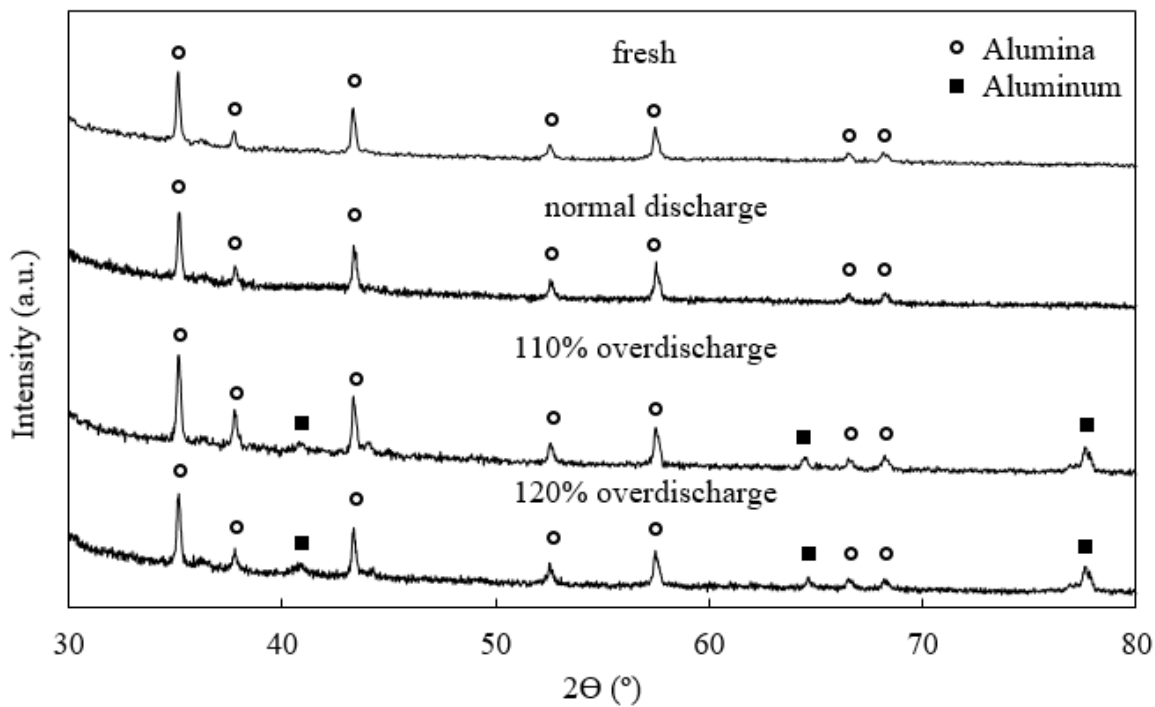
Fig. 6 SEM image of the separator under 120% over-discharge condition. EDX line and area scan results are shown in the image.

X-ray diffraction was conducted to reveal the compositional change inside the separator after over-discharging. The XRD patterns for the fresh separator, and the separators under normal discharge, 110% over-discharge and 120% over-discharge conditions are shown in Fig. 7 (a) and (b). Before  $30^\circ$ , the peaks of polyethylene, which is the major composition of the separator, were shown. Meanwhile, some alumina peaks were found in both cycled and uncycled separators. This implies that the alumina was not formed inside the separator during the charge and discharge process, and it was coated inside the separator during the manufacturing process. It is noted that

around  $41^\circ$ ,  $65^\circ$  and  $78^\circ$ , the aluminum peaks exist for the separators under 110% and 120% over-discharge conditions, while no aluminum was found for the fresh separator and the separator under normal discharge condition. This suggests the aluminum was formed inside the separator under over-discharge conditions.



(a)



(b)

Fig. 7 XRD patterns for fresh separator, and separators under normal, 110% and 120% over-discharge conditions. (a)  $2\theta$  ranges from  $10^\circ$  to  $80^\circ$ ; (b)  $2\theta$  ranges from  $30^\circ$  to  $80^\circ$ . The XRD patterns were zoomed in to make alumina and aluminum peaks more visible.

Combined XRD patterns with the SEM images and EDX results, it can be concluded that pure aluminum was formed in the separator during the over-discharge process, which has not been observed in the literatures. It seems that under high temperature, the alumina in the separator was reduced and formed pure aluminum. However, this reduction reaction is still unknown and needs further investigation. Once the pure aluminum accumulates and connects with each other, an electron-conducting channel will be formed inside the separator. The occurrence of aluminum will cause micro short circuit, which leads to the failure of the cells. In order to prevent the internal

short circuit during over-discharging, other ceramic material needs to be used as additives to the separator instead of aluminum. Such ceramic additives should have high temperature tolerance and good chemical stability inside the battery.

#### **4. Conclusions**

In this paper, the over-discharge effect on commercial 18650 NMC cells was studied. The cell skin temperature was monitored during the over-discharge process. The results show the temperature arises with the increase of over-discharge cycles, indicating strong exothermal reactions happened inside the cell. The SEM images clearly show melted regions in the separator under 110% over-discharge condition, suggesting internal short circuit occurred in the cell. The EDX results combined with XRD patterns reveal that pure aluminum formed in the separator. The aluminum may be the product of reduction reaction of alumina. The chemical reaction mechanism is still unknown. To avoid internal short circuit during over-discharging, a new ceramic additives to the separator is need to replace alumina. Such ceramic material needs to endure high temperature during over-discharging and have good chemical stability inside the battery.



## References

- [1] J. M. Tarascon and M. Armand, *Nature*, **414**, 359 (2001).
- [2] J. B. Goodenough and K. S. Park, *J. Am. Chem. Soc.*, **135**, 1167 (2013).
- [3] "Thinkpad Battery Recall," *Lenovo support*, August, 2007.
- [4] "Tesla Fires Raise Doubts About Seemingly Untouchable Company," *ABC News*, November, 2013.
- [5] "Dreamliner Battery Probe Ends: 8 Questions And Answers," *CNN News*, December 2014.
- [6] P. Ping, Q. Wang, P. Huang, K. Li, J. Sun, and D. Kong, *J. Power Sources*, **285**, 80 (2015).
- [7] C. F. Lopez, J. A. Jeevarajan, and P. P. Mukherjee, *J. Electrochem. Soc.*, **162**, A2163 (2015).
- [8] F. Larsson and B. E. Mellander, *J. Electrochem. Soc.*, **161**, A1611 (2014).
- [9] J. Lamb and C. J. Orendorff, *J. Power Sources*, **247**, 189 (2014).
- [10] H. Wang, S. Simunovic, H. Maleki, J. N. Howard, and J. A. Hallmark, *J. Power Sources*, **306**, 424 (2016).
- [11] E. Sahraei, J. Meier, and T. Wierzbicki, *J. Power Sources*, **247**, 503 (2014).
- [12] C. K. Lin, Y. Ren, K. Amine, Y. Qin, and Z. Chen, *J. Power Sources*, **230**, 32 (2013).
- [13] M. Hashimoto, M. Yamashiro, T. Ichihashi, A. Toda, T. Miyazaki, and S. Fujieda, *ECS Trans.*, **69**, 17 (2015).
- [14] H. F. Jin, Z. Liu, Y. M. Teng, J. k. Gao, and Y. Zhao, *J. Power Sources*, **189**, 445 (2009).

- [15] Y. Zheng, K. Qian, D. Luo, Y. Li, Q. Lu, and B. Li, *RSC Adv.*, **6**, 30474 (2016).
- [16] S. I. Tobishima, K. Takei, Y. Sakurai, and J. I. Yamaki, *J. Power Sources*, **90**, 188 (2000).
- [17] H. He, Y. Liu, Q. Liu, Z. Li, F. Xu, and C. Dun, *J. Electrochem. Soc.*, **160**, A793 (2013).
- [18] M. Gauthier, T. J. Carney, A. Grimaud, L. Giordano, N. Pour, and H. H. Chang, *J. Phys. Chem. Lett.*, **6**, 4653 (2015).
- [19] A. M. Andersson, K. Edström, N. Rao, and Å. Wendsjö, *J. Power Sources*, **81**, 286 (1999).